

Recognition and classification for surface defects of Si₃N₄ ceramic bearing inner ring based on RetinaNet method and NAM attention mechanism

Nanxing WU¹, Dahai LIAO¹, Zhihui CUI¹, Xin ZHANG¹, Wenjie LI¹, and Qi ZHENG²

¹Laboratory of Ceramic Material Processing Technology Engineering Jiangxi 333403 PR China)

²Jingdezhen Ceramic Institute

June 18, 2022

Abstract

Due to surface defects on inner ring of Si₃N₄ ceramic bearing are tiny and difficult to detect, the defects accelerate the wear of ceramic parts and reduce the performance of ceramic parts. A surface defect detection method based on RetinaNet method and NAM attention mechanism is proposed. Besides, the performance of RetinaNet method and Faster RCNN method is compared. The platform for surface defects of Si₃N₄ ceramic bearing inner ring is built independently to collect images. The dataset is made up of collected images and expanded by online data augmentation. Resnet-50 is used as the feature extraction network. The NAM attention mechanism is added to the tail of Resnet-50 to form an attention module to improve the model accuracy. As the bounding box regression loss function, loss is used for learning bounding box regression and localization uncertainty. A multi-scale feature pyramid is constructed by a feature pyramid network to integrate multi-level feature information. And a small full convolutional network is used as a classification sub-network and a bounding box regression sub-network. The results show that the mAP of the method reaches 91.84%, which is 13.45% and 2.1% higher compared to Faster RCNN and RetinaNet, respectively. The method has good detection effect on the identification and classification of surface defect species.

Recognition and classification for surface defects of Si₃N₄ ceramic bearing inner ring based on RetinaNet method and NAM attention mechanism

LIAO Dahai^{1,2#}, CUI Zhihui^{1,2#}, ZHANG Xin², LI Wenjie², ZHENG Qi¹, WU Nanxing^{1,2*}

(1.School of Mechanical and Electronic Engineering, Jingdezhen Ceramic University, Jingdezhen, People's Republic of China)

(2. Laboratory of Ceramic Material Processing Technology Engineering, Jiangxi 333403, PR China)

Abstract: Due to surface defects on inner ring of Si₃N₄ ceramic bearing are tiny and difficult to detect, the defects accelerate the wear of ceramic parts and reduce the performance of ceramic parts. A surface defect detection method based on RetinaNet method and NAM attention mechanism is proposed. Besides, the performance of RetinaNet method and Faster RCNN method is compared. The platform for surface defects of Si₃N₄ ceramic bearing inner ring is built independently to collect images. The dataset is made up of collected images and expanded by online data augmentation. Resnet-50 is used as the feature extraction network. The NAM attention mechanism is added to the tail of Resnet-50 to form an attention module to improve the model accuracy. As the bounding box regression loss function, loss is used for learning bounding box regression and localization uncertainty. A multi-scale feature pyramid is constructed by a feature pyramid network to integrate multi-level feature information. And a small full convolutional network is used as a classification sub-network and a bounding box regression sub-network. The results show that

the mAP of the method reaches 91.84%, which is 13.45% and 2.1% higher compared to Faster RCNN and RetinaNet, respectively. The method has good detection effect on the identification and classification of surface defect species.

Keywords: Si₃N₄ ceramic bearing inner ring, RetinaNet, Online data augment, NAM attention mechanism, Surface defects detection

1 Introduction

Si₃N₄ ceramic materials have high mechanical properties such as low coefficient of thermal expansion, heat resistance, corrosion resistance and wear resistance^[1]. Ceramic materials also have thermal, electrical and chemical properties^[2]. As a result, ceramic bearings are widely used in aerospace engines, biomedical devices and transportation. Since the process of ceramic products is susceptible to factors such as mixing and sintering, they are prone to external defects^[3]. The main types of defects are pit, crack, wear and snowflake^[4], which affect the performance of ceramic materials. The defects of ceramic products are relatively small and difficult to be recognized by the human eye. At present, the inspection methods for surface defects of ceramic materials at home and abroad are mainly divided into two methods: manual inspection and nondestructive testing. Manual inspection method test results have the disadvantages of low detection efficiency, high false detection rate, randomness, and poor stability. Non-destructive testing (NDT)^[5-7] is a method for detecting the type, number, shape, location and size of surface defects in ceramic materials without changing the surface or internal structure of the ceramic.

With the rapid development of artificial intelligence (AI) and machine learning, convolutional neural networks (CNNs) have been widely used in computer vision. Such as object detection, student teaching^[8], health analysis, etc. Aiming at the vehicle navigation light guide plate (LGP) image characteristics, Li et al^[9] proposed a visual detection method based on improved RetinaNet. They proposed and used an improved feature pyramid network module to improve the feature fusion network in the retinal network. Experimental results show that the method is effective. In the vehicle LGP data set, the average detection rate is 98.6%. Mingming Zhu^[10] et al. proposed a RetinaNet-based method for detecting arbitrarily oriented ships. By a rotated RetinaNet, a refined network, a feature alignment module, and an improved loss function, rotated detection, achieving better detection progress and solving boundary discontinuity are achieved to locate ships with high accuracy. Yantong Chen^[11] et al. proposed a fly species recognition method based on the refined RetinaNet and the convolutional block attention module (CBAM). A multi-scale feature pyramid was constructed. Kullback-Leibler (KL) loss superseded smoothed L1 loss for simultaneously learning bounding box regression and localization uncertainty. The method achieves an average accuracy (mAP) of 90.38%, which is better than existing methods. The average time to identify a single image is 0.131s.

Combining NDT techniques with deep learning methods to process Si₃N₄ ceramic bearing inner ring surface defect images, online data augmentation is used to expand the images and form the dataset. Attention mechanisms SE, CBAM and NAM are added to the tail of the Resnet-50 feature extraction network, respectively. It is found that the NAM attention mechanism improves the model recognition and classification accuracy most significantly by comparison. Improved loss function replaces Smooth L1 loss for learning bounding box regression and uncertain localization. The Si₃N₄ ceramic bearing inner ring surface defect recognition and classification model is obtained by training the network for testing surface defects. The main contributions of this paper are as follows: the platform for surface defects of Si₃N₄ ceramic bearing inner ring is built independently to collect surface defects images, the online data augmentation is used to expand the surface defect dataset, adding NAM to obtain a more complete attention map and better global information of the image. The results show that the proposed method has better performance compared with the Faster RCNN and RetinaNet.

The rest of this paper is organized as follows. Chapter 2 introduces the platform for surface defects of Si₃N₄ ceramic bearing inner ring. Chapter 3 presents the Si₃N₄ ceramic bearing inner ring surface defect analysis and dataset fabrication. Chapter 4 introduces the Si₃N₄ ceramic bearing inner ring surface defect identification and classification model. Chapter 5 outlines the experimental results and analyzes the

feasibility of the proposed method. Chapter 6 presents the conclusion.

2 Si_3N_4 ceramic bearing inner ring surface defects identification and classification platform construction

The prerequisite for analyzing and predicting surface defects inside the inner ring of Si_3N_4 ceramic bearings using deep learning models is a large-scale dataset. To produce a Si_3N_4 ceramic bearing inner ring surface defect dataset, the surface defect images are collected by building a non-destructive inspection platform. The inspection platform is composed of feeding module, image acquisition module and image processing module. The feeding module includes mechanical arm, coaxial rotating gear and motor. The image acquisition module consists of high-speed CCD camera, stereo microscope and LED light source. The image processing module includes image acquisition card, image memory card and industrial PC.

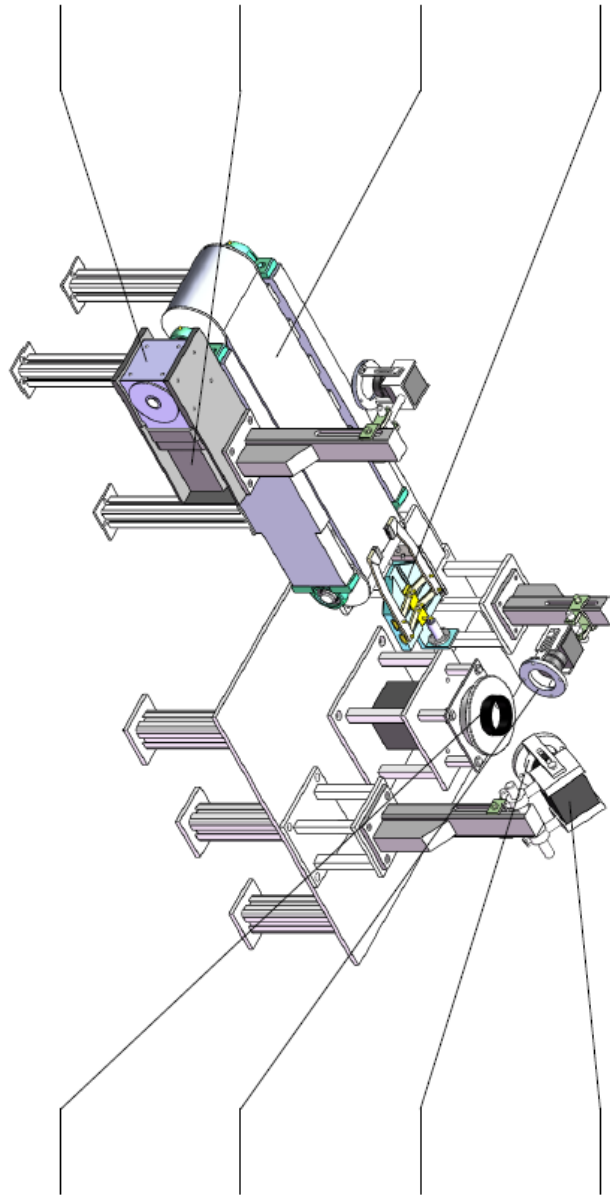


Fig.1 Schematic diagram of platform for surface defects of Si_3N_4 ceramic bearing ring

Driven by the motor and acted by the reducer, the Si_3N_4 ceramic bearing sample is transferred by the coaxial transmission device. And the mechanical arm transfers the sample to the image acquisition module to complete the feeding process. The stereo microscope magnifies the tiny defects on the surface of Si_3N_4 ceramic bearing inner ring, the hemispherical LED light source provides sufficient light. The high-speed CCD camera acquires the surface defect images. The collected defects are connected to the industrial PC via image acquisition card and image memory card, respectively through bus and serial port.

3 Si_3N_4 ceramic bearing inner ring surface defect analysis and dataset production

3.1 Surface defect analysis

During the preparation process, due to abrasive friction, insufficient purity of raw materials and sintering temperature, the surface of Si_3N_4 ceramic bearing is prone to defects, such as pit, snowflake, wear and crack defects. On account of the formation of volatile substance CO , pores are left on the surface of ceramics. As the oxidation temperature increases to 1100°C , grains with dendritic shapes begin to form and grow, and the growth process of dendritic grains will fill the pores and heal the crack defects formed during the heating process^[12]. Si_3N_4 ceramics are subjected to extrusive external forces during grinding and polishing processes. The grinding disc is directly squeezed and abrasive grains are pressed into the ceramic under the action of the grinding disc, forming pit defects^[13]. Ceramic materials are brittle, and wear defects remain on the surface of ceramic materials due to severe abrasive wheel wear^[14]. In the polishing process of Si_3N_4 ceramics, the material removal process mainly includes plastic deformation, brittle fracture and powdering of the surface material. The plastic deformation and powdering of surface materials lead to the generation of snow defects^[15].



Fig. 2 Analysis of surface defects of Si_3N_4 ceramic bearings roller inner ring

The pixel 3D map of Si_3N_4 ceramic bearing inner ring surface defect image is drawn by python programming

language, as shown in Figure 2. The distribution of surface defects is observed through the pixel 3D map. Figure 2(e1-e4) represents the pixel 3D map of pit, wear, snowflake and crack defects respectively, and the distribution locations of defects are marked in the map.

3.2 Surface defect image processing

Image marking

A prerequisite for deep learning models to achieve better image recognition and classification results is a large-scale dataset of labeled training sets [16]. LabelIMG is a free, open source graphical image annotation tool. The LabelIMG tool is used to label the training set with the labels of pits, wears, snowflakes and cracks. A digital image of the Si₃N₄ ceramic bearing inner ring surface defects is acquired and an annotation file is output. The file comes with an interactive drawing containing the borders of all pixels of the Si₃N₄ ceramic bearing inner ring surface defects, with bounding boxes drawn around each identified defect in the image.

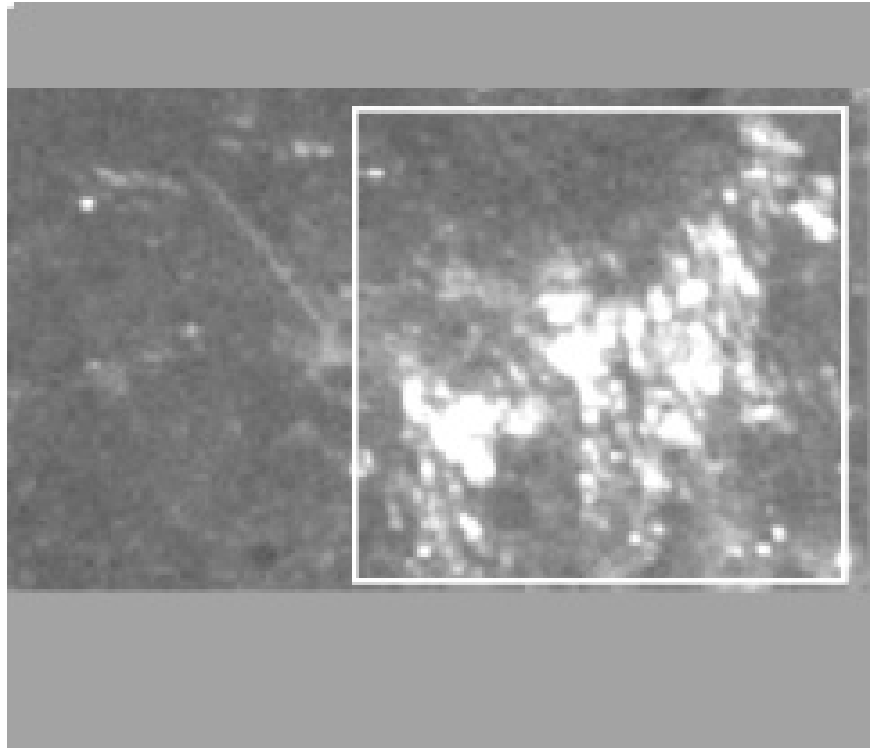


Fig. 3 Online data augmentation expansion dataset

Data augmentation

Large-scale datasets can enhance the generalization ability^[17] and robustness of target detection models^[18]. The effects of data enhancement are as follows: Increase the amount of data for training to improve the generalization ability of the model. Increase the noisy data to improve the robustness of the model and avoid overfitting^[19]. Data augmentation can be divided into two categories: offline augmentation, online augmentation. Online augmentation enhances the acquired batch data, such as rotation, translation, folding, etc. And is used in the case of a larger dataset size.

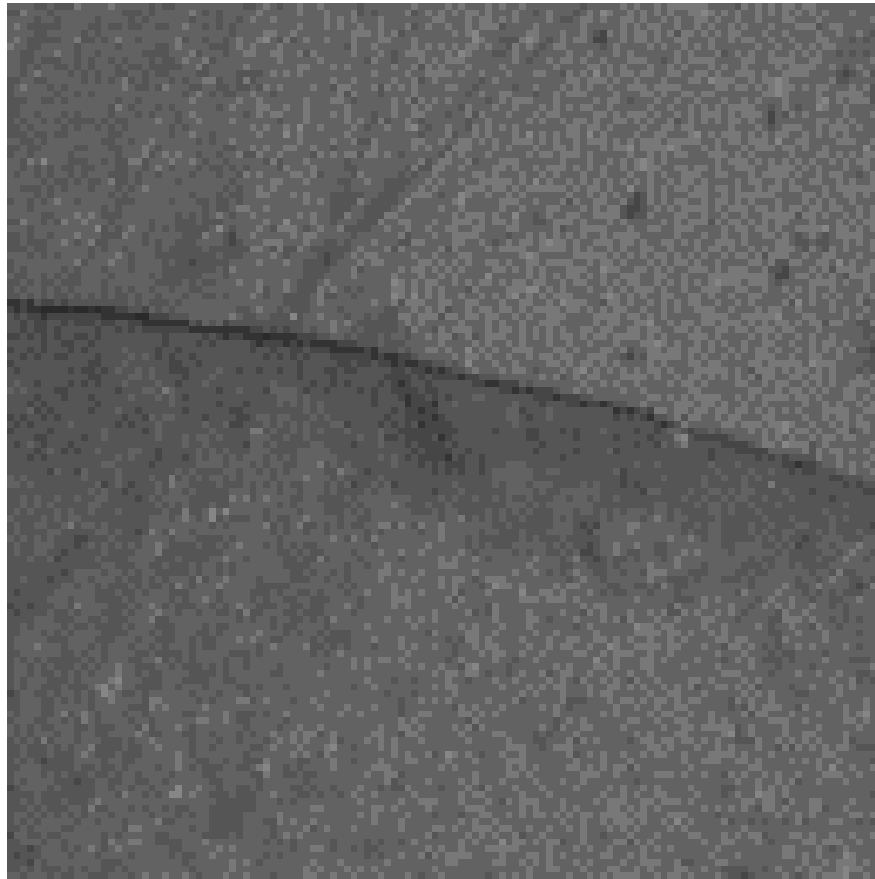
In this paper, online augmentation is used to expand the surface defect dataset, and the online data enhanced image is shown in Figure 3. After data augmentation, surface images are obtained and divided into training data set, validation data set and test data set according to the ratio of 7:2:1.

Tab 1 Table of data set size and number of defects

Type of defect	Pit	Crack	Wear	Sanowflake	Total
Training database	385	385	385	385	1540
Testing database	55	55	55	55	220

4 Si₃N₄ ceramic bearing inner ring surface defect identification and classification model

The experimental platform of Si₃N₄ ceramic bearing inner ring surface defect image detection is built by ourselves, and the surface defect images are obtained and made into dataset. As shown in Figure 4, the completion of surface defect recognition and classification is divided into four processes, which are preprocessing and Labelling, data augmentation, feature extraction and defects classification recognition.



A-Preprocessing and Labelling, B-Data augmentation, C- Feature extraction, D-Defects classification recognition

Fig. 4 Flow chart of surface defect identification and classification of Si₃N₄ ceramic bearing inner ring

Preprocessing and labeling, the prerequisite for deep learning models to obtain better recognition and classification results is labeling the training set [20]. The contrast between the defective part and the background is enhanced by image preprocessing. LabelIMG is used to mark the surface defects, which are Pit, Crack, Wear and Snowflake. The XML file corresponding to the defect is generated. It is used to store the information

of Si_3N_4 ceramic bearing roller inner ring surface defect, including the location, name, shape and boundary frame information of the defect. The boundary frame contains the pixel information of the surface defect.

Data augmentation, large-scale dataset is beneficial to obtain better recognition and classification results. Online data augmentation expands the size of the dataset, improves the robustness of the target detection model, prevents the occurrence of overfitting.

Feature extraction, the expanded data set is input from the input layer to the convolutional neural network and output from the output layer. And it is subsequently passed through CONV layer, pooling layer, CONV layer, pooling layer and fully connected layer. The images are transformed into two-dimensional matrices. Image features are preliminary extracted. Statistical features are extracted and image features are recorded according to regions.

Defects classification recognition, smaller feature matrix is got. The features of each part are summarized. ReLU activation function is used to output feature values. The process of surface defect image recognition and classification has been completed.

4.1 Faster RCNN model

Based on SPPnet and Fast RCNN, Ren, S. et al. ^[21]introduced a region proposal network (RPN). RPN shares full image convolution features with the detection network. As shown in Figure 5, Fater RCNN completes the surface defect recognition and classification by three processes: feature extraction, extraction of suggestion frames and classification.

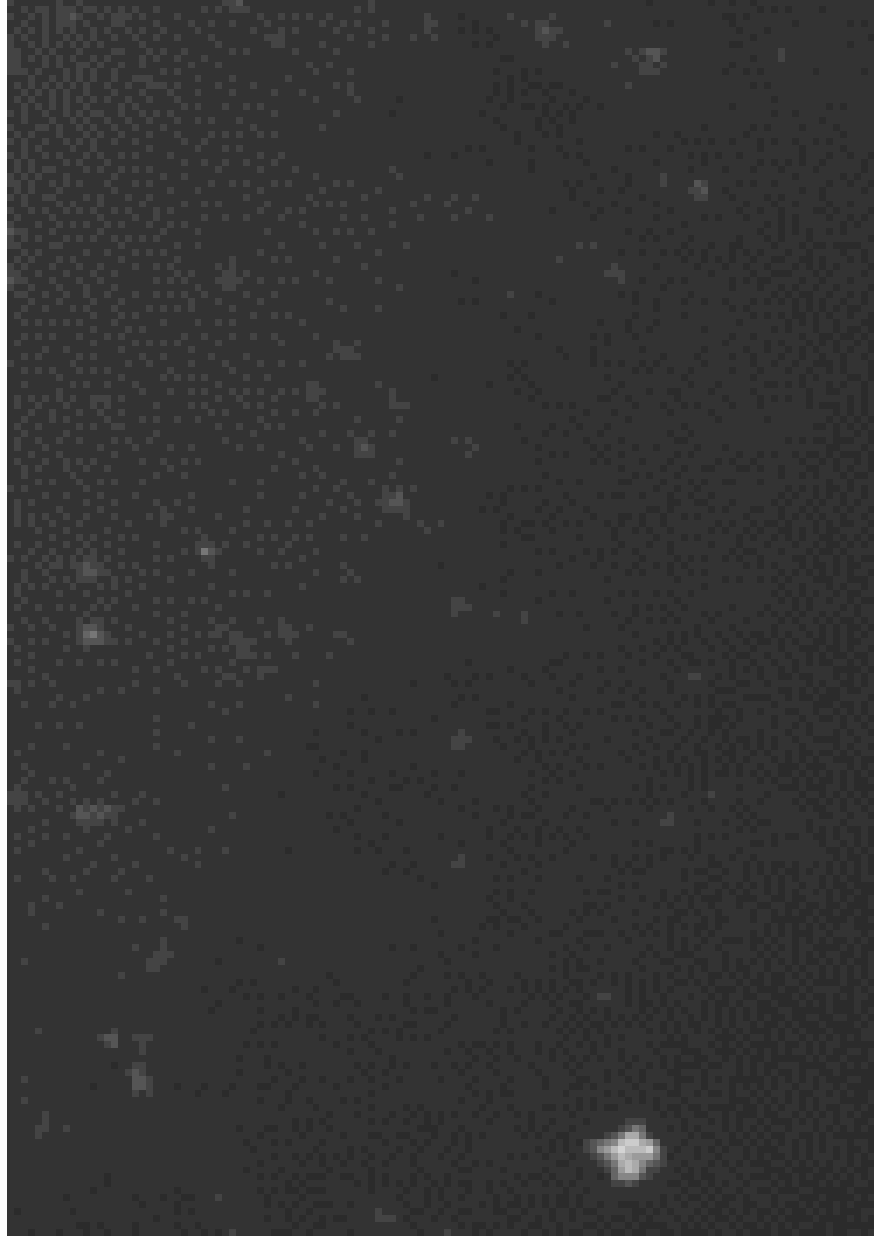


Fig. 5 The diagram of Faster R-CNN framework

The defect image of the input model is extracted by 13 CONV layers, 13 ReLU layers and 4 pooling layers. The feature map of the surface defect image is extracted using a set of basic CONV+ReLU+pooling layers for the subsequent RPN layers and fully connected layers.

4.2 RetinaNet model

Since the one-stage detector is not as accurate as the two-stage detector, T. -Y. Lin et al. [22] proposed a new loss function: focal loss and designed a dense detector: RetinaNet. By reducing the weight of the easily classified samples to pay more attention to the difficult-to-classify samples, the RetinaNet can achieve not only the speed of the first-level detector, but also the accuracy of the second-level detector. RetinaNet

is essentially composed of resnet residual network, FPN with two FCN sub-networks. The structure of RetinaNet model is shown in Figure 7.

4.3 Improvement of RetinaNet model

NAM attention mechanism

Liu Yc et al. [23] proposed a new normalization-based attention module (NAM), which suppresses insignificant weights. It applies a weight sparsity penalty to the attention modules, thus improving their computational efficiency while maintaining similar performance. Comparison with SE, BAM, and CBAM attention mechanism on Resnet and Mobilenet, it has been shown that the NAM attention mechanism has higher accuracy.

The NAM attention mechanism is a lightweight and efficient attention mechanism, and the channel attention submodule of NAM is shown in Figure 6. The input feature layer pixels are normalized and convolved with the weights, and the feature layer is output by sigmoid. For the channel attention sub-module, the scaling factor BN in Batch Normalization is used, as in equation . The scaling factor reflects the size of the variation of each channel and indicates the weight of that channel. The scaling factor is the variance in BN. The larger the variance, the more the channel varies, then the richer the information contained in that channel will be and the greater the weight. To suppress the unimportant features, a regularization term is added to the loss function.

μ_B is the mean of mini batch B and σ_B is the standard deviation of mini batch B. γ and β are trainable affine transformation parameters (scale and shift).

The improved loss function is shown in Equation (2). x denotes the input. y is the output. W is the network weight. $g(\gamma)$ is the L1 parametric penalty function. P is the penalty that balances $g(\gamma)$ and $g(\lambda)$.

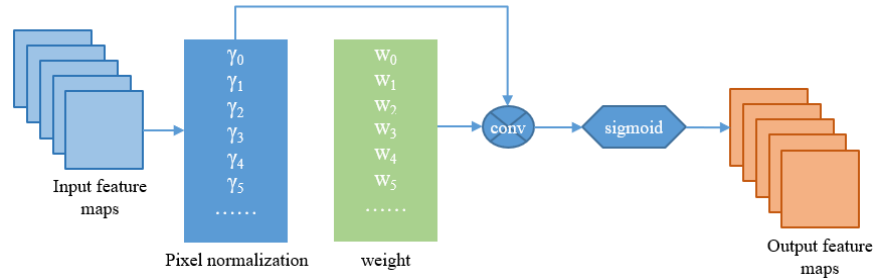


Fig. 6 The diagram of NAM attention mechanism framework

RetinaNet model refinement

As a lightweight, high-performance attention mechanism, the NAM attention mechanism is plug-and-play. The NAM attention module is inserted into the tail of the ResNet-50 and connected to the head of the multiscale object detection algorithm: FPN to form the attention module, as shown in the yellow part in Figure 7. Thus, the improved RetinaNet model has been formed.

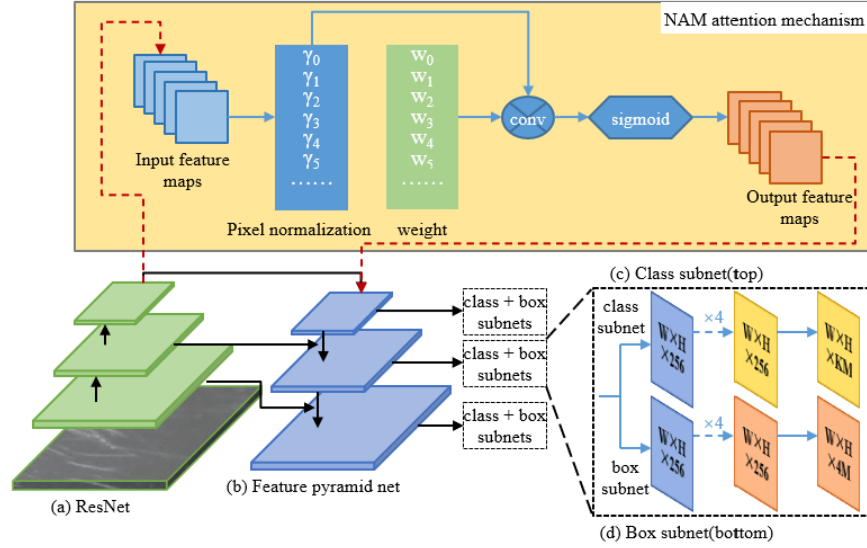


Fig. 7 The diagram of the improved RetinaNet model framework

FPN solves the multi-scale problem in object detection by simply connecting the network. The performance of surface microdefect detection has been substantially improved with essentially no increase in the computational effort of the original model. Top-down connections are made through top-level features for upsampling and low-level features, and predictions are made at each level. The more abstract and semantic high-level feature map is collected. And the low-resolution feature map is upsampled as 2 times nearest neighbor to generate the feature map using the underlying localization information. Thus, the target box category classification and bbox location regression tasks are completed. The surface defect recognition and classification tasks are realized to classify surface defects as pit, crack, snowflake and wear.

4.4 Evaluation criteria of model

Accuracy is the ratio of the number of correctly classified samples to the total number of samples. The higher the accuracy, the better the model performance.

Precision refers to the proportion of positive samples predicted by the model, which reflects the model's ability to distinguish negative samples. The higher the Precision value, the higher the model accuracy.

Recall represents the proportion of all positive samples in the test set that are correctly identified as positive samples. and represents the ability of the classifier to find all positive samples.

F1-score is the harmonic mean of precision and recall. The higher the F1-score, the more robust the model is.

Where TP is positive samples correctly identified as positive samples. TN indicates negative samples correctly identified as negative samples. FP refers to false positive samples, that is., negative samples incorrectly identified as positive samples. FN indicates false negative samples, that is, positive samples incorrectly identified as negative samples.

AP refers to the average precision, which is the area under the PR curve. The better the model, the higher the AP value.

The mAP is the average of multiple class APs and takes the range of [0,1]. The larger the value the better the model performance.

Where, n denotes the number of defect types on the surface of Si_3N_4 ceramic bearing inner ring, that is, $n=4$. i denotes the defect type, and the value is [0,3].

The performance of the improved RetinaNet model is verified using the Si_3N_4 ceramic bearing inner ring surface defect dataset. The model performance evaluation results are shown in Table 2. The improved RetinaNet model performs well on the dataset with a Recall value of 92.59%, which is close to 1, an F1-score value of 0.95, a precision value of 98.19%, and a mAP value of 91.84%. Pit has an AP value of 100%, Crack has an AP value of 79.11%, Wear has an AP value of 96.43%, and snowflake has an AP value of 91.82%. Pit and snowflake have the highest recall value, both at 100.00%. Wear had the second highest recall value, at 96.43%. Crack has the lowest recall value, at 73.91%. Pit has the highest F1-score value of 1.00. Wear has the second highest F1 value of 0.98. Snowflake has an F1 value of 0.95. And crack has the lowest F1 value of 0.85. Pit, crack and wear all have a precision value of 100.00% and snowflake had a precision value of 90.91%.

Tab 2 Evaluation results of the improved RetinaNet on surface defect dataset of Si_3N_4 ceramic bearing inner

Type of defect	Recall	F1-score	Precision	AP	mAP
Pit	100.00%	1.00	100.00%	100.00%	/
Crack	73.91%	0.85	95.85%	79.11%	/
Wear	96.43%	0.98	100.00%	96.43%	/
Snowflake	100.00%	0.95	96.91%	91.82%	/
All	92.59%	0.95	98.19%	/	91.84%

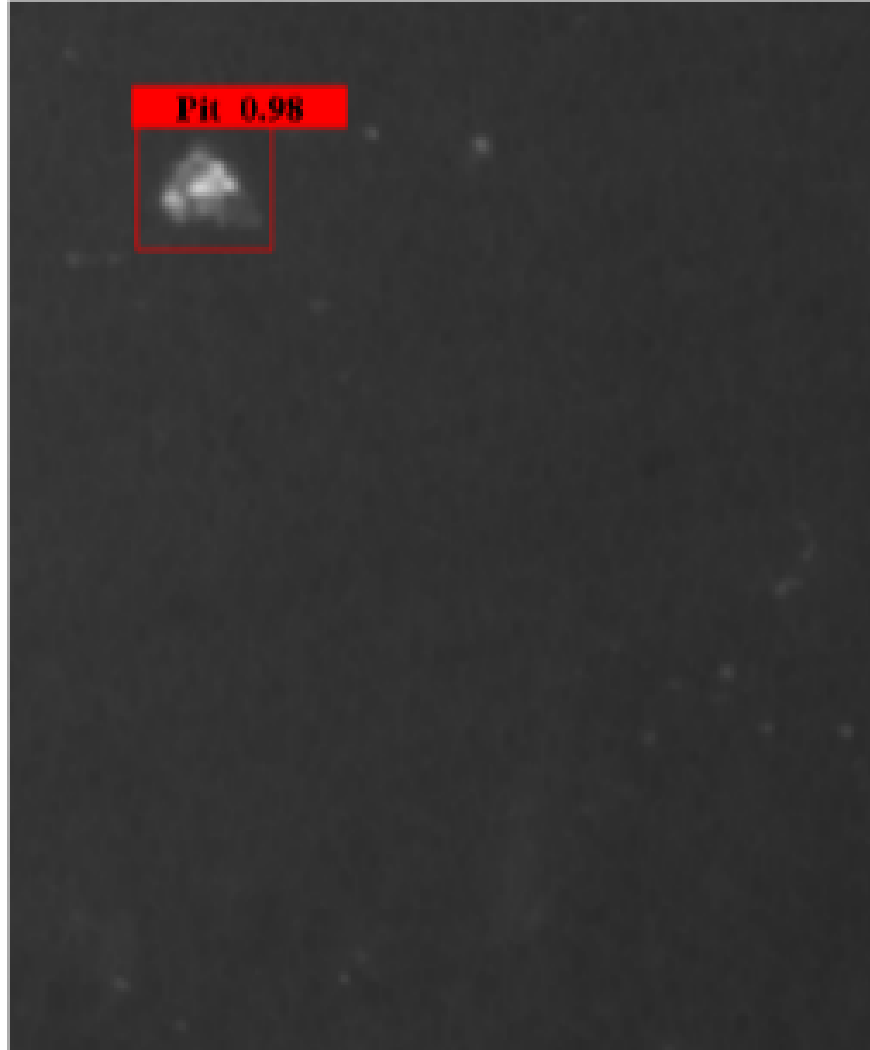


Fig. 8 Predicted results of the improved RetinaNet for Si₃N₄ ceramic bearing ring surface defect dataset

Using the improved RetinaNet model for the verification set of defects on the surface of Si₃N₄ ceramic bearings, the prediction results are shown in Figure 8. The red, green, purple and blue boxes in the figure represent the prediction boxes for pit, Wear, crack and snowflake, respectively. The prediction results of some defect images are shown in this figure. The prediction values of Pit are 0.98, 0.95, 0.99, and 0.98. The prediction values of wear are 1.00, 1.00, 0.99, and 0.99. The prediction values of Crack are 0.99, 0.96, 0.99, and 1.00. The prediction values of snowflake are 0.96, 0.88, 0.94, and 0.95. From the figure, the prediction performance of the improved RetinaNet for the validation set of surface defects is shown.

5 Experimental results and analysis

mAP value comparison

In this paper, the performance of Faster RCNN, RetinaNet and improved RetinaNet are compared. The model comparison results are shown in Table 3. The mAP values for backbone of Faster RCNN using vgg, resnet and adding CBAM are 78.39%, 77.71% and 78.41%. The mAP values of RetinaNet, RetinaNet with SE, CBAM and improved RetinaNet are 89.74%, 89.69%, 90.80% and 91.84%, respectively. The results show that the mAP values of the improved RetinaNet are improved by 13.45% and 2.1%, respectively, compared

to the Faster RCNN and RetinaNet.

Tab 3 mAP value comparison of models

Model	mAP
Faster RCNN(vgg)	78.39%
Faster RCNN(resnet)	77.71%
Faster RCNN+CBAM	78.41%
RetinaNet	89.74%
RetinaNet+SE	89.69%
RetinaNet+CBAM	90.80%
Improved RetinaNet	91.84%

loss curve

A good model should not only have high accuracy but also good generalization ability. Poor generalization ability of the model leads to overfitting. The model's mAP is plotted as shown in Figure 9(b). It is proved that precision of the model has been improved.

The model parameters are adjusted to improve the model's generalization ability while improving the model's accuracy. The model's loss curves as shown in Figure 9(a) are drawn. By visualizing the channel feature graph, the content of each channel is represented by binary images to judge the performance of the convolution kernel. The training process of the model is divided into three stages, namely, the stage of substantial decline, the stage of small decline and the stage of keeping convergence. In the stage of substantial decline, the learning rate drops by gradient, and then the loss curve changes to the stage of slight decline. When learning reaches a certain stage, the loss curve region is stable and begins to converge. Figure 9(a1) shows the loss curve of Faster RCNN. The model is iterated for 150 times. As the number of iterations increases, the loss curve decreases continuously until it becomes stable and convergent. The feature maps of A1, B1 and C1 correspond to the stage of substantial decline, the stage of small decline and the stage of keeping convergence respectively. Figure 9(a2) shows the loss curves of the RetinaNet model with 300 iterations. A2, B2 and C2 feature maps correspond to the stage of substantial decline, the stage of small decline and the stage of keeping convergence respectively.

The improved RetinaNet model is used to predict the validation set of the surface defect dataset. Precision and recall values are obtained. P-R curve is drawn, as shown in Figure 10. The horizontal axis of the P-R curve is recall and the vertical axis is precision. Under a certain threshold value, the model determines that the results greater than the threshold value are positive samples, and those less than the threshold value are negative samples. The points on the curve represent the recall rate and accuracy rate corresponding to the returned results. The origin represents the precision and recall of the model when the threshold is maximum. Models with high Precision and low Recall are not able to complete some tasks requiring precise positioning. Models with low Precision and high Recall are characterized by low model recognition rate.

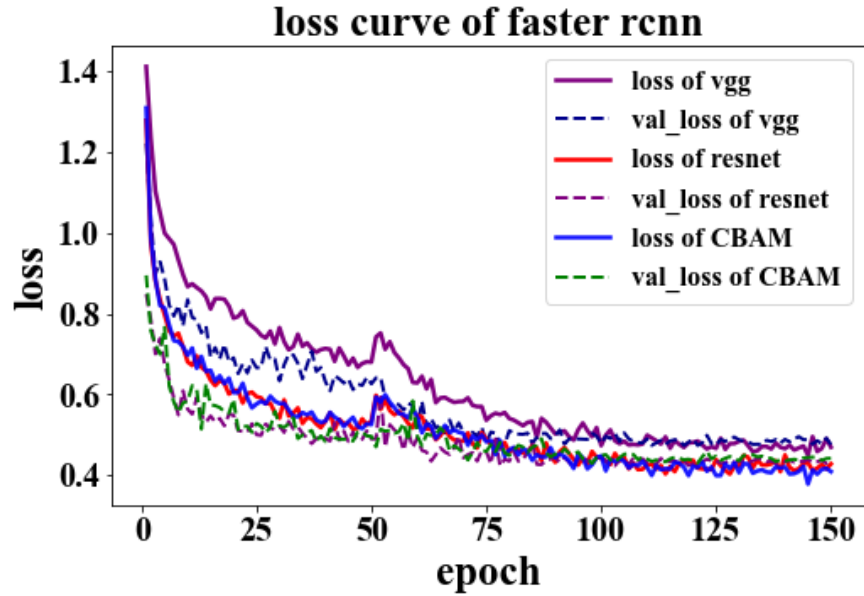


Fig. 9 Comparison chart between model Loss curve and model mAP value

P-R curve

The pink, purple, green and gold curves in the figure represent the P-R curves of pit, wear, snowflake and crack respectively. The P-R curves of pit completely cover the P-R curves of crack, which indicates that the improved RetinaNet model has better prediction performance for pit than that of crack. Wear’s P-R curve intersects with Snowflake’s. Predictive performance is compared by equilibrium points. The P-R curve of snowflake has break-event Point (BEP) A, and the P-R curve of wear has BEP B. Precision at points A and B is equal to recall. Point B is larger than point A, indicating that the prediction performance of improved RetinaNet model for wear is better than that of snowflake. The order of defect prediction performance is pit, wear, snowflake and crack.

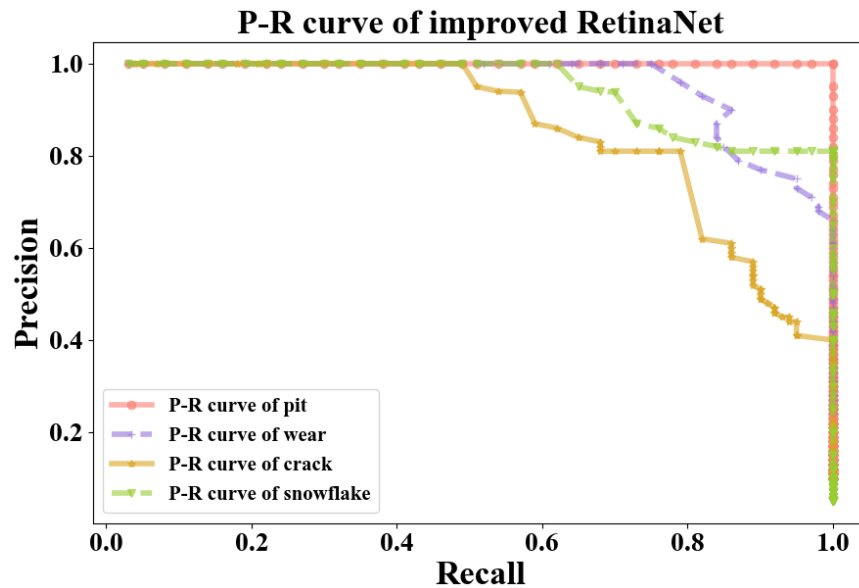


Fig. 10 P-R curve of surface defects on Si₃N₄ ceramic bearing inner ring

6 Conclusion

In this paper, the Faster RCNN model and the RetinaNet model are studied. The surface defects of Si₃N₄ ceramic bearing inner ring are taken as the research object. The backbone of the RetinaNet model is ResNet-50. The performance of RetinaNet model is improved by comparing Faster RCNN with RetinaNet. SE, CBAM and NAM attention modules are added to the tail of ResNet to form attention modules. Comparing the effects of different attentional modules on model performance, NAM attentional module has the most significant effect on model performance. NAM attentional module is used to form improved RetinaNet model.

The surface defects images are collected by the platform established by ourselves and made into dataset by LabelIMG. The online data augmentation is used to expand the surface defect dataset of Si₃N₄ ceramic bearing inner ring. The improved Faster RCNN model and RetinaNet model are used to train the surface defect dataset and verify the model performance. This improved RetinaNet has the characteristics of high precision in pit, wear, crack and snowflake detection, and is superior to Faster RCNN model. Compared with the Faster RCNN model and the RetinaNet model, the mAP value of the improved RetinaNet model increased by 13.45% and 2.1%, respectively.

Disclosure statement

No potential conflict of interest is reported by the author(s).

Funding

This work is supported by Jiangxi Youth Foundation [grant number 2021A A B 214033], the Key Foundation of Jiangxi Province of China [grant number 2021A C B 204012] and the National Natural Science Foundation of China [grant number: 51964022].

Reference

1. W. Wang, Yao, D., Liang, H.: Novel silicothermic reduction method to obtain Si₃N₄ ceramics with enhanced thermal conductivity and fracture toughness. *Journal of the European Ceramic Society* . (2020)
2. H. Q. R. C.C. Ye, C.P. Zhang.: Fracture toughness of Si₃N₄ ceramic composites: Effect of texture. *Journal of the European Ceramic Society* . 41(13), 6346-6355. (2021)
3. H. L. Huihui Zhang, Haibo Wu.: Microwave absorbing property of gelcasting SiC-Si₃N₄ ceramics with hierarchical pore structures. *Journal of the European Ceramic Society* . 42(4), 1249-1257. (2022)
4. N. J. T.H. Tsaia, C.H. Yang.: Non-destructive evaluations of 3D printed ceramic teeth: young's modulus and defect detections. *Ceramics International* . 46(14), 22987-22998. (2020)
5. Zhike Zhao.: Review of non-destructive testing methods for defect detection of ceramics. *Ceramics International* . 47(4), 4389-4397. (2021)
6. T. T. F. Sakamoto. Prediction of strength based on defect analysis in Al₂O₃ ceramics via non-destructive and three-dimensional observation using optical coherence tomography. *Journal of the Ceramic Society of Japan* . 127(7), 462-268, (2019)
7. A Noori Hoshyar Rashidi, M. Liyanapathirana R.: Algorithm Development for the Non-Destructive Testing of Structural Damage. *Applied Sciences* . 9(14), 2810-2832. (2019)
8. L. S. Nur Baiti Afini Normadhi, Hairul Nizam Md Nasir, Andrew Bimba.: Identification of personal traits in adaptive learning environment: Systematic literature review. *Computers & Education* . 130, 168-180. (2019)
9. H. W. Junfeng Li.: Surface defect detection of vehicle light guide plates based on an improved RetinaNet. *Measurement Science and Technology* . 33(4). (2022)
10. M. a. H. Zhu, Guoping Zhou, Hao Wang.: Arbitrary-Oriented Ship Detection Based on RetinaNet for Remote Sensing Images. *IEEE Journal of Selected Topics in Applied Earth Observations and Remote Sensing* . 14, 6694-6704. (2021)

11. X. Z. Y. Chen, W. Chen, Y. Li, J. Wang.: Research on Recognition of Fly Species Based on Improved RetinaNet and CBAM. *IEEE Access* . 8, 102907-102919. (2020)
12. X. Y. Hanqin Liang, Zhengren Huang, Yuping Zeng.: The relationship between microstructure and flexural strength of pressureless liquid phase sintered Sic ceramics oxidized at elevated temperatures. *Ceramics International* . 42(11), 13256-13261. (2016)
13. W. L.-q. YANG Tie-bin, GU Le.: Processing Defect Analysis and Nondestructive Evaluation Technology for Si3N4 Bearing Ball. *ACTA ARMAMENTARII* . 28(13), 353-357. (2007)
14. S. Y. Guochao Qiao, Wei Zheng, Ming Zhou.: Material removal behavior and crack-inhibiting effect in ultrasonic vibration-assisted scratching of silicon nitride ceramics. *Ceramics International* . 48(3), 4341-4351. (2022)
15. X. Xiao, Jiayun Deng, Qiang Xiong: Scratch Behaviour of Bulk Silicon Nitride Ceramics. *Micromachines* . 12(6), 707-719. (2021)
16. J. Li, Changchun Li, Shuaipeng Fei, Wheat Ear Recognition Based on RetinaNet and Transfer Learning. *Sensors* . 21(14), 4845-4866. (2021)
17. Su, Q., Wang, H., Xie, M, et al.: Real-time traffic cone detection for autonomous driving based on YOLOv4. *IET Intell. Transp.Syst.* 1-11(2022)
18. A. Kamilaris, Prenafeta-Boldú, F. X.: Deep learning in agriculture: A survey. *Computers and Electronics in Agriculture* . 147, 70-90. (2018)
19. S. Demir, Mincev, K., Kok, K., & Paterakis, N. G., "Data augmentation for time series regression: Applying transformations, autoencoders and adversarial networks to electricity price forecasting", *Applied Energy* . vol. 304, pp. 117695-117714, 2021
20. Q. Xie, Zhang, P., Yu, B., et al.: Semisupervised Training of Deep Generative Models for High-Dimensional Anomaly Detection. *IEEE Transactions on Neural Networks and Learning Systems* . 1-10. (2021)
21. S. Ren, He, K., Girshick, R., & Sun, J.: Faster R-CNN: Towards Real-Time Object Detection with Region Proposal Networks. *IEEE Transactions on Pattern Analysis and Machine Intelligence* . 39(6), 1137-1149. (2017)
22. P. G. T. -Y. Lin, R. Girshick, K. He: Focal loss for dense object detection. *IEEE Transactions on Pattern Analysis and Machine Intelligence* . 42(2), 318-328. (2020)
23. Z. S. Yichao Liu, Yueyang Teng, Nico Hoffmann.: NAM: Normalization-based Attention Module. *arXiv - CS - Computer Vision and Pattern Recognition* . (2021)